

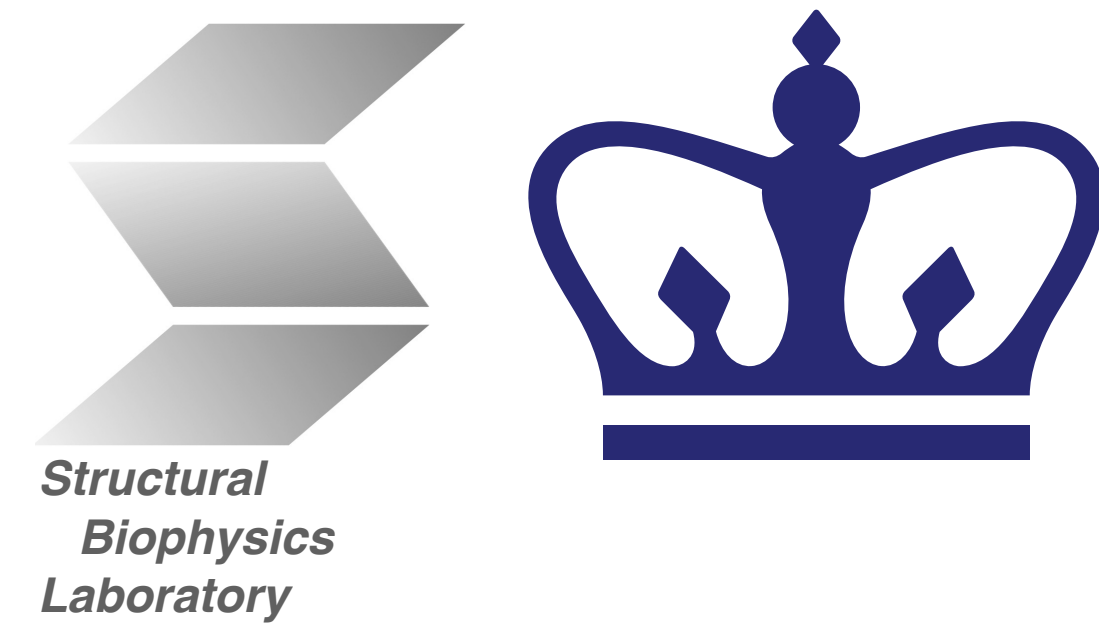


Dynamics of GCN4 Facilitate DNA Interaction: A Model-Free Analysis of an Intrinsically Disordered Region

Michelle L. Gill,¹ R. Andrew Byrd,¹ Arthur G. Palmer²

¹Structural Biophysics Laboratory, National Cancer Institute, Frederick, MD 21702

²Department of Biochemistry and Molecular Biophysics, Columbia University Medical Center, New York, NY 10032



Introduction

Intrinsically disordered proteins (IDPs) and proteins with intrinsically disordered regions (IDRs) are known to play important roles in regulatory and signaling pathways. A critical aspect of these functions involves the formation of highly specific complexes with target molecules.

Using NMR spin relaxation parameters (¹⁵N R₁, R₂, and {¹H}-¹⁵N heteronuclear NOE) collected at four static magnetic fields (14.1, 16.5, 18.8, and 21.1 T), the backbone dynamics of the basic leucine-zipper (bZip) domain of the *S. cerevisiae* transcription factor GCN4 have been analyzed. Model-free analysis was applied to *apo* GCN4, significantly extending previous NMR studies of GCN4 dynamics performed using a single static magnetic field of 11.74 T [1]. These results are verified using a novel spectral density mapping technique and correlate well with molecular dynamics simulations [2].

In contrast to the earlier work, data at multiple static fields allows the time scales of internal dynamics of GCN4 to be quantified. Large amplitude dynamic fluctuations in the DNA-binding region have correlation times ($\tau_s \approx 1.4\text{--}2.5$ ns) that are consistent with a two-step mechanism in which partially ordered conformations of GCN4 form initial encounter complexes with DNA and then rapidly rearrange to the high affinity state with fully formed basic region recognition helices.

These results are described in Gill, et. al, *Phys. Chem. Chem. Phys.*, 2016, 18, 5839–5849 [3].

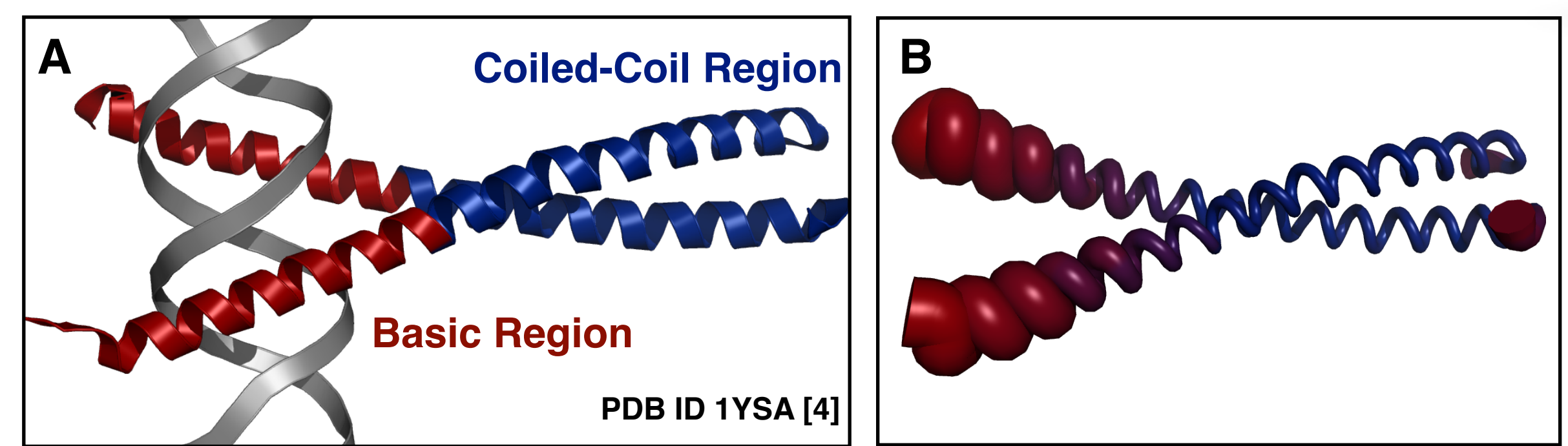


Figure 1. (A) The DNA binding domain of GCN4 contains an N-terminal basic region (red) and a C-terminal coiled-coil region (blue). (B) The basic region is disordered in the absence of DNA, as demonstrated by the order parameters (S^2) determined by Bracken, et. al [1].

¹⁵N Amide Spin Relaxation Parameters

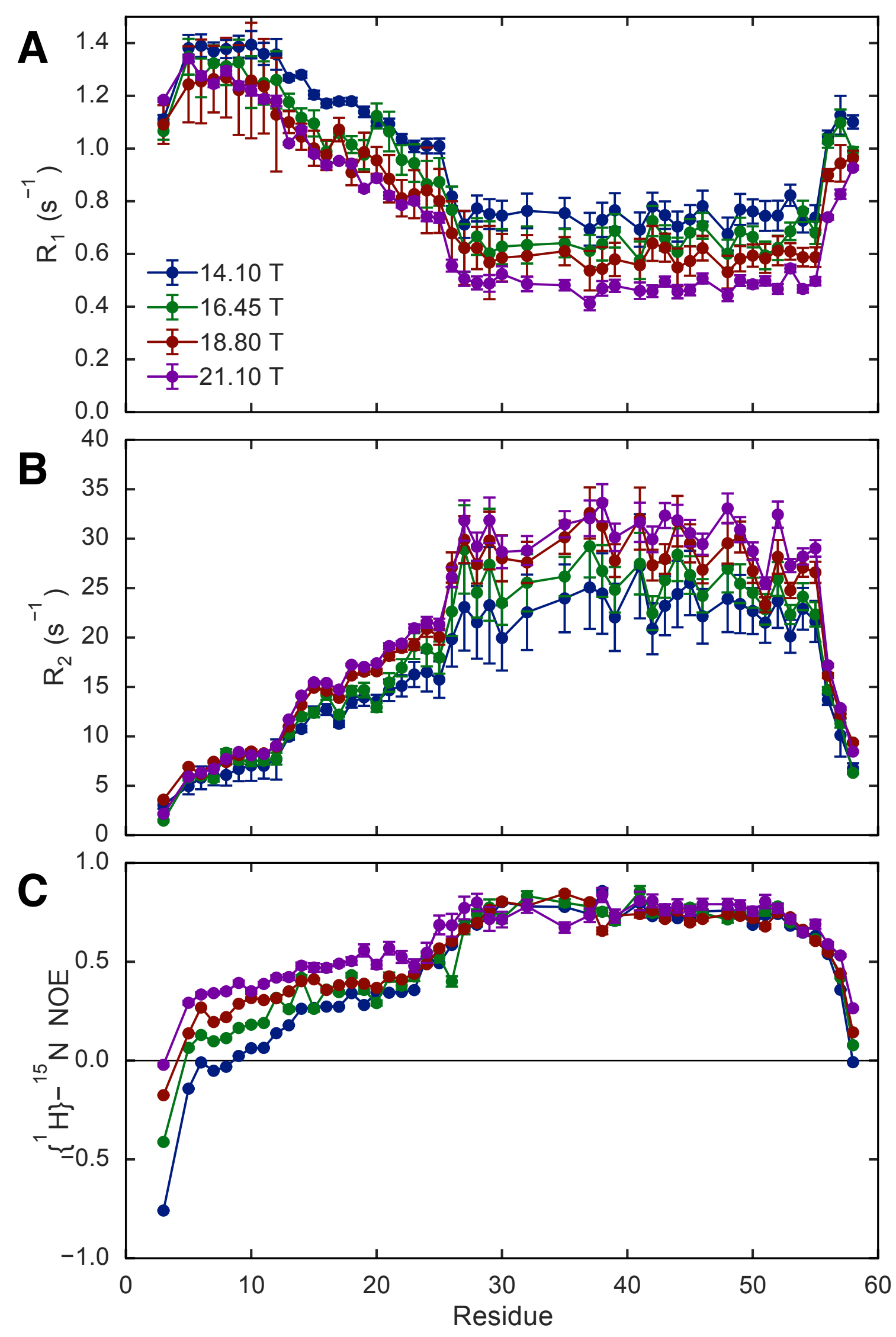


Figure 2. The ¹⁵N amide spin relaxation parameters (A) R₁, (B) R₂, and (C) {¹H}-¹⁵N heteronuclear NOE were determined at four static fields: 14.10, 16.45, 18.80, and 21.10 T, shown in blue, green, red, and purple, respectively.

Model-Free Analysis

$$\begin{aligned} \text{Model 0 } J(\omega) &= \frac{2}{5}\tau_m \\ \text{Model 1 } J(\omega) &= \frac{2}{5} \left[\frac{S^2\tau_m}{1 + \omega^2\tau_m^2} \right] \\ \text{Model 2 } J(\omega) &= \frac{2}{5} \left[\frac{S^2\tau_m}{1 + \omega^2\tau_m^2} + \frac{(1-S^2)\tau_e'}{1 + \omega^2\tau_e'^2} \right] \\ \text{Model 5 } J(\omega) &= \frac{2}{5} \left[\frac{S^2\tau_m}{1 + \omega^2\tau_m^2} + \frac{(S_f^2 - S^2)\tau_s'}{1 + \omega^2\tau_s'^2} \right] \\ \text{Model 6 } J(\omega) &= \frac{2}{5} \left[\frac{S^2\tau_m}{1 + \omega^2\tau_m^2} + \frac{(S_f^2 - S^2)\tau_s'}{1 + \omega^2\tau_s'^2} + \frac{(1-S_f^2)\tau_f'}{1 + \omega^2\tau_f'^2} \right] \end{aligned}$$

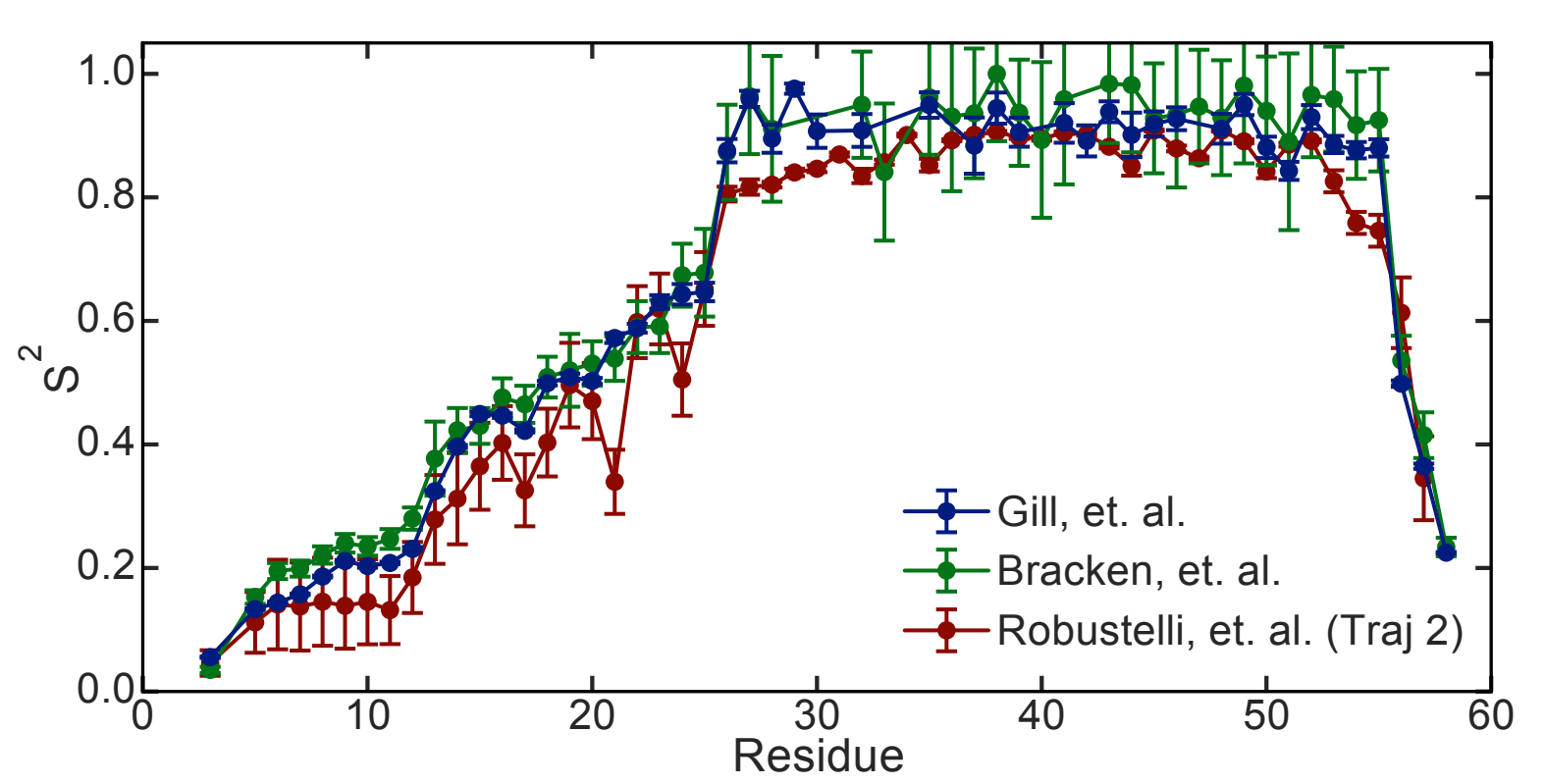
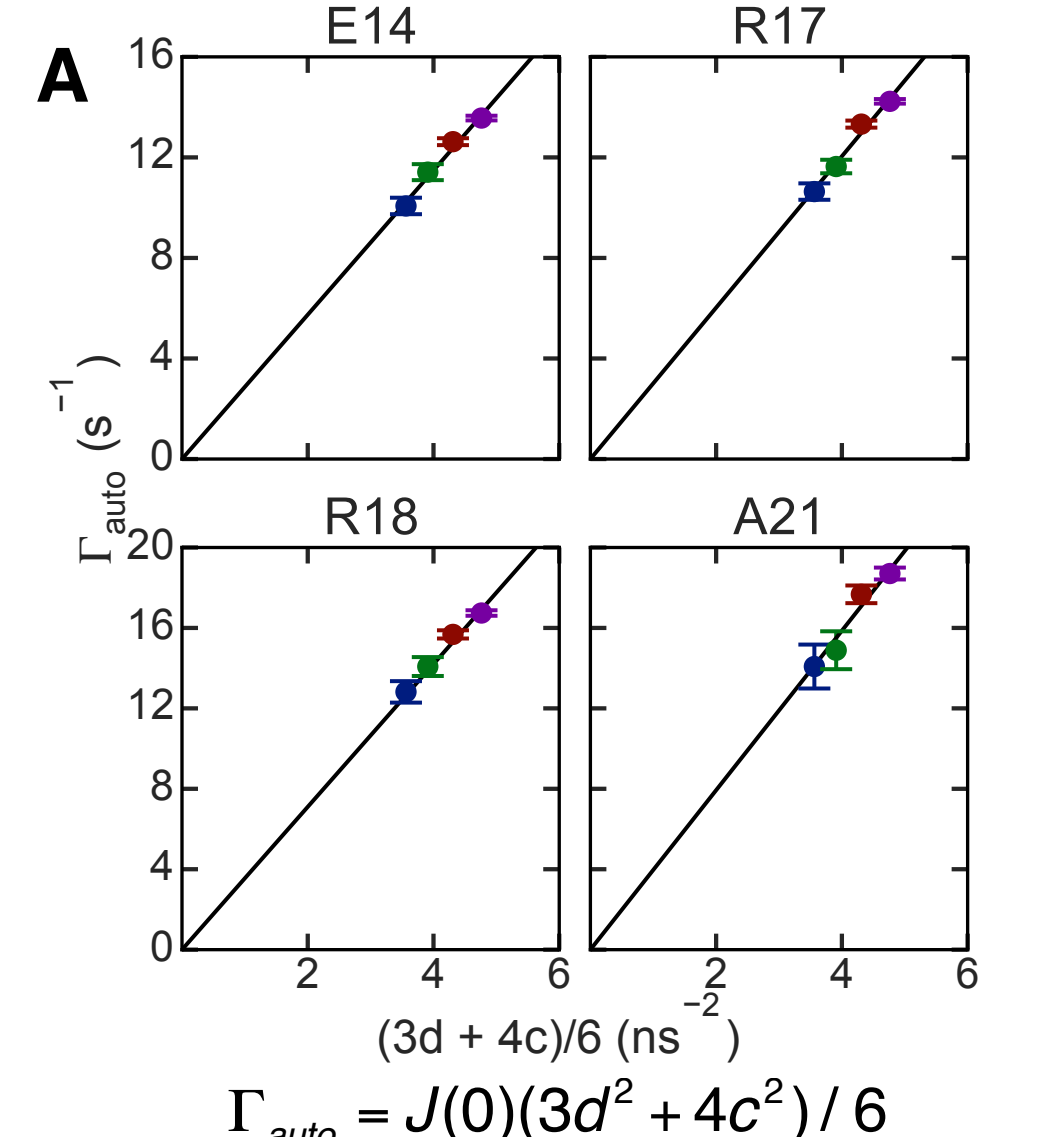


Figure 3. Model-free analysis was performed using five different models and the resulting order parameters (S^2 , blue) compare well with those previously measured [1] (green) and determined from simulations [2] (red).

Spectral Density Mapping (I)

$$\begin{aligned} \text{Calculate } \Gamma_{\text{auto}}, J(\omega_N), J(0.870\omega_H) \text{ from NMR data} \\ \Gamma_{\text{auto}} = R_2 - 0.5R_1 - 0.454\sigma_{NH} \\ J(\omega_N) = (R_1 - 1.249\sigma_{NH}) / (3d^2 / 4 + c^2) \\ J(0.870\omega_H) = 4\sigma_{NH} / (5d^2) \\ \text{Perform linear regressions using } \Gamma_{\text{auto}} \text{ and Model 6} \\ \Gamma_{\text{auto}} = J(0)(3d^2 + 4c^2) / 6 \\ J(\omega) = \frac{2}{5} \left[\frac{S^2\tau_m}{1 + \omega^2\tau_m^2} + \frac{(S_f^2 - S^2)\tau_s'}{1 + \omega^2\tau_s'^2} + \frac{(1-S_f^2)\tau_f'}{1 + \omega^2\tau_f'^2} \right] \\ \text{Assume time scale separation: } \tau_m \gg \tau_s \gg \tau_f \end{aligned}$$



$$\begin{aligned} J(0.870\omega_H) &= m_H(0.870\omega_H)^{-2} + b_H \\ m_H &= \frac{2}{5}[S^2/\tau_m + (S_f^2 - S^2)/\tau_s'] \\ b_H &= \frac{2}{5}(1-S_f^2)\tau_f' \\ J(\omega_N) &= m_N\omega_N^{-2} + b_N \\ m_N &= \frac{2}{5}S^2/\tau_m \\ b_N &= \frac{2}{5}[(S_f^2 - S^2)\tau_s' + (1-S_f^2)\tau_f'] \end{aligned}$$

Figure 4. Spectral density mapping was performed using the method of Mayo, et. al [5], where the parameters are determined from linear regressions of (A) Γ_{auto} , (B) $J(0.870\omega_H)$, and (C) $J(\omega_N)$. Select residues from the basic domain are shown in A–C.

Spectral Density Mapping (II)

$$\begin{aligned} S^2 &= \frac{5}{2}[(J(0) - b_N)m_N]^{1/2} \\ \tau_m &= [(J(0) - b_N)/m_N]^{1/2} \\ S_f^2 &= S^2 + \frac{5}{2}[(b_N - b_H)(m_H - m_N)]^{1/2} \\ \tau_f' &= \frac{5}{2}b_H/(1-S_f^2) \\ \tau_s' &= [(b_N - b_H)/(m_H - m_N)]^{1/2} \end{aligned}$$

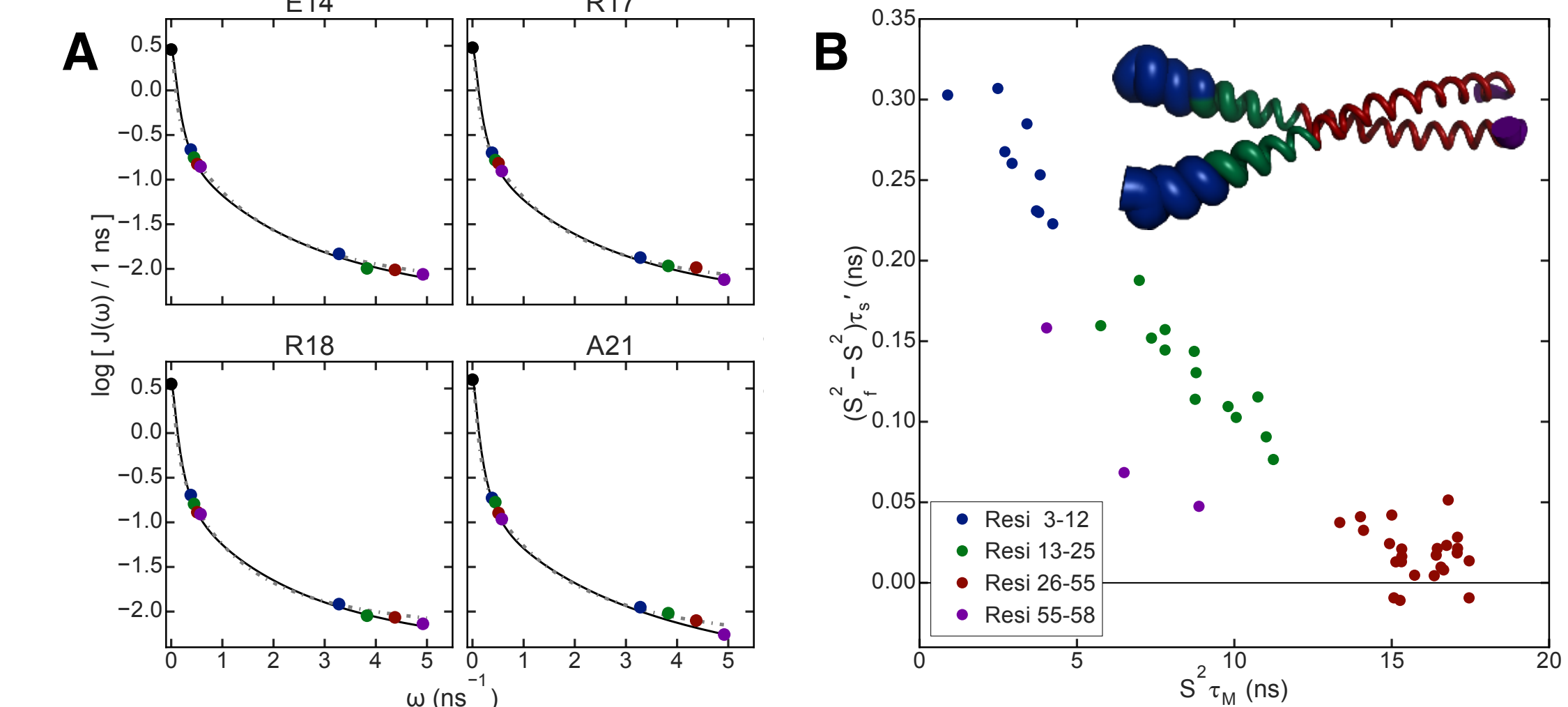


Figure 5. Parameters from the linear regressions were used to calculate S^2 , τ_m , S_f^2 , τ_f' , and τ_s' . (A) Spectral density curves from Model-free (dashed, gray line) analysis and spectral density mapping (black, solid line) are shown for select residues from the basic domain. (B) Regions of GCN4 cluster based on dynamical parameters.

Comparison

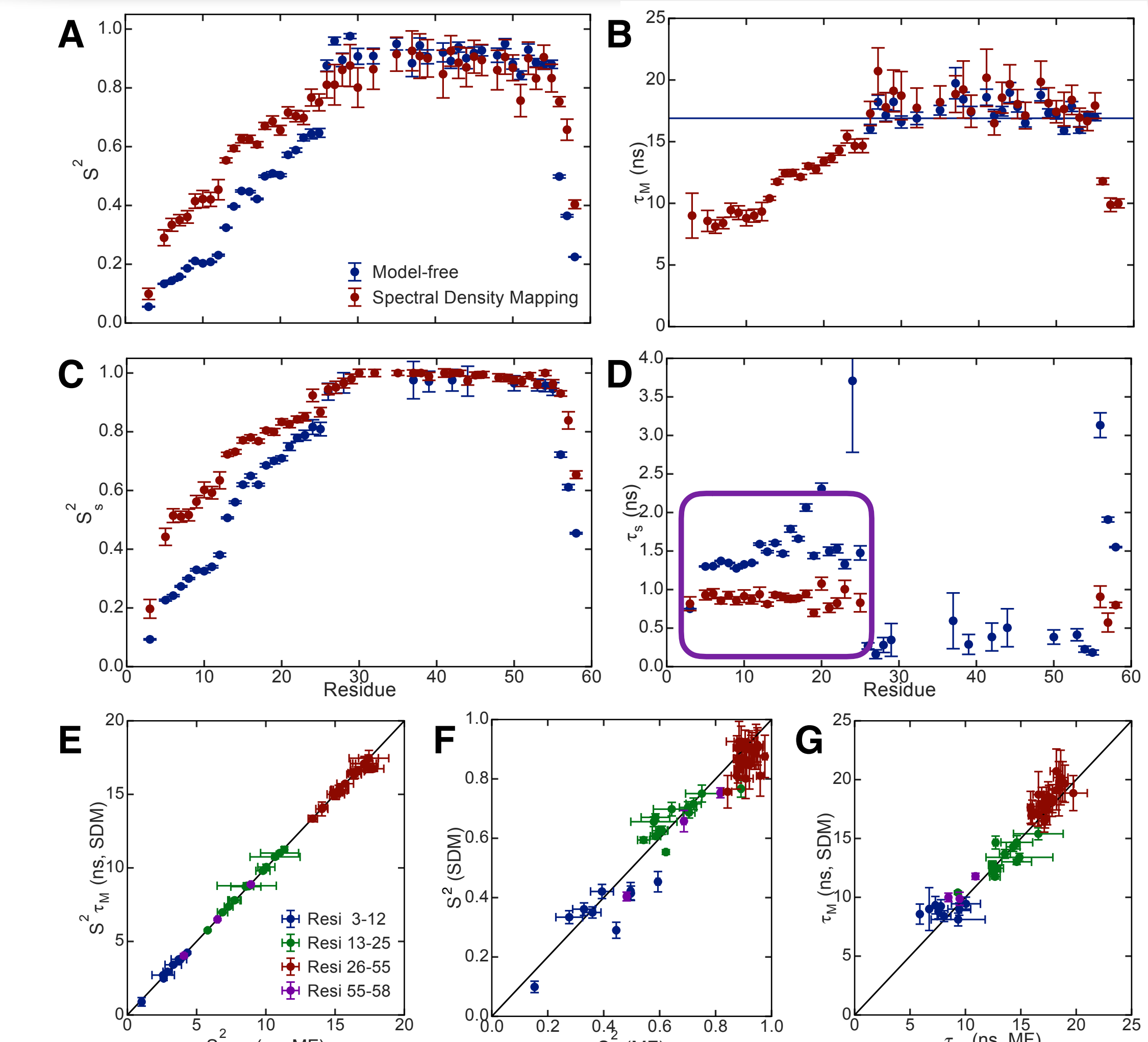


Figure 6. Comparison of dynamical parameters from Model-free (blue) analysis and spectral density mapping (red) for global motions, (A) S^2 and (B) τ_m , and internal motions, (C) S_f^2 and (D) τ_s' . (E–G) Global motions determined from Model-free (MF) analysis and spectral density mapping (SDM) cluster by protein region.

Conclusions

- The correlation time of slow internal motions (τ_s , 1.4–2.5 ns) is faster than both the estimated binding rate of GCN4 to DNA and the experimentally determined off-rate
- Slow internal motions could facilitate encounter complex formation and subsequent rearrangement upon substrate binding
- Indicates possible subsequent roles for conformational selection and induced fit

References

- Bracken C., Carr P.A., Cavanagh J. & Palmer A.G. (1999) *J. Mol. Biol.*, **285**, 2133–2146.
- Robustelli P., Trbovic N., Friesner R.A. & Palmer A.G. (2013) *J. Chem. Theory Comput.*, **9**, 5190–5200.
- Gill M.L., Byrd R.A. & Palmer A.G. (2016) *Phys. Chem. Chem. Phys.*, **18**, 5839–5849.
- Ellenberger T.D., Brandl C.J., Struhl K. & Harrison S.C. (1992) *Cell*, **71**, 1223–1237.
- Mayo K.H., Daragan V.A., Idrisatullin D. & Nesmelova I. (2000) *J. Mag. Res.*, **146**, 188–195.

Acknowledgments

This work was supported by NIH grants GM50291 and GM089047 to AGP and MLG, respectively. The data acquired at 16.45, 18.8, and 21.1 T were collected at NYSBC, which was made possible by a NYSTAR grant and ORIP/NIH facility improvement grant CO6RR015495. The 900 MHz NMR spectrometers were purchased with funds from NIH grant P41GM066354. This research was partially supported by the Intramural Research Program of the National Cancer Institute.